

1 **Supporting Information**

2
3
4
5 **Methane emissions from Pantanal, South America, during the low water**
6 **season: Towards more comprehensive sampling**

7
8
9 David Bastviken^{1*}, Ana Lucia Santoro², Humberto Marotta², Luana Queiroz Pinho²,
10 Debora Calheiros³, Patrick Crill⁴, Alex Enrich-Prast²

11
12
13
14 ¹ Department of Thematic Studies – Water and Environmental Studies, Linköping
15 University, 58183 Linköping, Sweden. E-mail: david.bastviken@liu.se. Phone: +46 13
16 282291.

17
18 ² Department of Ecology, Federal University of Rio de Janeiro, 68020 Rio de Janeiro,
19 Brazil. E-mail: aeprast@biologia.ufrj.br

20
21 ³ Center for Agricultural Research in the Pantanal – Embrapa Pantanal, Caixa Postal 109.
22 Corumbá – MS, Brazil. 79.320-900 E-mail: debora@cpap.embrapa.br

23
24 ⁴ Department of Geology and Geochemistry, Stockholm University, 10691 Stockholm,
25 Sweden. E-mail: patrick.crill@geo.su.se.

26
27 *Corresponding author
28

29
30 **This supporting information contains seven pages, two tables, and three figures.**

31

32 **Methods**

33

34 *Methane flux measurements*

35 Measurements of CH₄ flux at each site were performed during a full 24 h period
36 using floating chambers as described by Bastviken et al. (1). The chambers were made of
37 7 L plastic buckets which were equipped with styrofoam floats to float with the edges
38 reaching 4 cm below the water surface. Each chamber covered an area of 0.043 m². A
39 hole was drilled at the top of the chamber and an 11 mm rubber stopper was put in the
40 hole. A piece of PVC tubing (25 cm long, 5 mm outer diameter, 3 mm inner diameter)
41 was inserted through the stopper in one end and attached to a luer-lock syringe valve at
42 the other end. The tubing facilitated sampling from the chambers by syringe with
43 minimal disturbance of the chamber position. The chambers were covered with
44 aluminum foil to reflect the sunlight and minimize internal heating. Each chamber was
45 attached to a separate styrofoam float by a 1 m line. This additional float was connected
46 to a stone with another line to anchor the chamber. When measuring in or next to
47 macrophyte stands, chambers were sometimes attached to plants above the water level to
48 avoid drifting.

49

50 For the 24 h measurements (8 to 34 chambers per lake), only initial and final
51 samples were taken. A 50 ml polypropylene plastic syringe (Becton Dickinson) equipped
52 with a polycarbonate stopcock was attached to the tubing leading to the chambers. The
53 syringe was pumped three times to mix the chamber content before withdrawing 50 ml of
54 gas from the chamber and closing the stopcock. Due to the remote location quick

55 analysis was not possible so the samples were transferred to storage vials. Vials were
56 prepared prior to sampling and consisted of 20 ml glass vials filled completely with
57 saturated NaCl and capped with a 10 mm thick butyl rubber stopper (Apodan, Denmark)
58 with an aluminum crimp seal. The NaCl brine in the vial was displaced through a second
59 needle when the sample was injected into the vial from the syringe. Previous tests
60 confirmed that CH₄ samples can be stored extended time periods in such vials. The
61 massive stoppers are thick enough to prevent leakage and the high concentration of NaCl
62 prevented both dissolution and oxidation of CH₄ in the remaining brine in the vials with
63 samples.

64

65 *Analyzes*

66 Concentrations of CH₄ in the storage vials were measured in the laboratory with a
67 GC-FID (Shimadzu 8A) equipped with a 500 µL injection loop and a 2 m x 3.2 mm
68 stainless steel column packed with HayeSep Q 80/100. The column oven temperature
69 was 40°C and the N₂ carrier gas pressure setting was 80 kPa which resulted in a column
70 flow of about 10 mL min⁻¹. Certified 99.9 ± 2 ppm, 1000 ± 20 ppm, and 1.95 ± 0.02 %,
71 CH₄ standards (Air Liquide) were used for calibration.

72

73 Lake water CH₄ concentrations samples were collected with a 50 ml plastic
74 syringe with the stopcock submerged a few centimeters below the water surface. After
75 rinsing with some water to remove air bubbles along the walls slightly more than 40 ml
76 of water was drawn into the syringe. A headspace equilibration method was used to
77 extract the CH₄ from the water (2). Water volume in the syringe was adjusted to 40 ml

78 and 20 ml of air was introduced into the syringe before closing the valve. Care was taken
79 to avoid breathing into the syringe. The syringe was shaken vigorously for 1 minute
80 which was tested to be enough to equilibrate the water with the headspace, and the
81 headspace was then transferred to a storage vial as described above. Air samples taken
82 at the same time were also transferred to storage vials to correct the measured headspace
83 concentration for the ambient CH₄ levels. The corrected headspace concentration was
84 used to account for the amount of CH₄ that remained dissolved in the sample syringe
85 using Henry's Law adjusted for temperature according to Wiesenburg and Guinasso (3).
86 The total amount of CH₄ in the sample syringe was calculated and this amount was then
87 divided by the water volume to obtain the surface water CH₄ concentration.

88

89 *Flux calculations*

90 The flux into the diffusion chambers was calculated as described in Bastviken et
91 al. (2004). The diffusive flux across the water surface into the floating chamber can be
92 described by the equation

93

$$94 \quad F = k(C_w - C_{fc}), \quad (1)$$

95

96 where F is the flux (moles m⁻² d⁻¹), k is the piston velocity (m d⁻¹), and C_w is the measured
97 CH₄ concentration in the water (moles m⁻³), and C_{fc} is the CH₄ concentration in the water
98 given equilibrium with the CH₄ partial pressure in the floating chamber (4). This
99 equation implies that the flux is driven by the concentration difference which will
100 decrease with time in the chambers. A simple calculation of the total amount of CH₄ that

101 entered the chambers divided with the time of measurement will underestimate the
102 instantaneous flux rate. To better estimate the instantaneous flux we solved for k .
103 Equation 1 was rewritten as

104

$$105 \quad \frac{(P_t - P_0) \cdot V}{R \cdot T \cdot A} = k \cdot (P_w \cdot K_h - P_0 \cdot K_h), \quad (2)$$

106

107 where P_t , and P_0 is the partial pressure of methane in the chamber (Pa) at times t and 0,
108 respectively, V is the chamber volume (m^3), R is the gas constant ($8.314 \text{ m}^3 \text{ Pa K}^{-1} \text{ mol}^{-1}$),
109 T is the temperature (K), A is the bottom area of the chamber (m^2), P_w is the partial
110 pressure of CH_4 in the chamber at equilibrium with C_w (Pa), and K_h is the Henry's Law
111 constant for CH_4 ($\text{moles m}^{-3} \text{ Pa}^{-1}$). Thereby,

112

$$113 \quad \frac{dP}{dt} = K \cdot (P_w - P), \text{ where} \quad (3)$$

114

$$115 \quad K = k \cdot \frac{K_h \cdot R \cdot T \cdot A}{V}. \quad (4)$$

116

117 The solution for Equation 3 is

118

$$119 \quad (P_w - P) = C \cdot e^{(K \cdot t)}, \quad (5)$$

120

121 where C is a constant determined by setting $t = 0$. After solving for k , the instantaneous
122 flux was calculated using Equation 1. The temperature dependence of K_h was calculated
123 from the Bunsen coefficients (3).

124

125 Ebullition was determined by subtracting the diffusive flux from the Diffusion
126 chambers from the total flux into the chambers without bubble shields. In many cases the
127 ebullition was extensive enough to result in chamber concentrations higher than the
128 equilibrium with CH_4 in the water. In such cases simple flux calculations (accumulated
129 CH_4 divided by chamber area and time) would underestimate fluxes due to diffusion of
130 CH_4 from the chamber into the water once the equilibrium concentration in the chamber
131 was passed. To compensate for this we made a simple mass balance model accounting
132 for diffusive flux (in any direction) over time in the chamber and estimating ebullition
133 rates by fitting the modelled chamber concentration to the measured final chamber
134 concentration. The average of the calculated piston velocity values (gas transfer
135 coefficient, k ; see Supporting Information) from the diffusion chambers on the same lake
136 and the water and chamber concentrations of CH_4 were used to calculate the diffusive
137 flux according the equation 1 in the supporting information. The average ebullition rate
138 during the whole measurement period was represented by a given constant rate for all
139 time steps in the model throughout the chamber deployment (since no data regarding
140 temporal variability between time steps were available). This assumption was supported
141 by the short term flux measurements indicating continuous ebullition (see results section).
142 If ebullition occurred in a non-continuous way our model would be biased for the
143 individual chambers. This would result in underestimated fluxes when most ebullition

144 occurred early during the measurement period, and overestimated fluxes for chambers if
145 ebullition occurred late in the deployment, but given random timing of the ebullition
146 events throughout the incubation periods the errors in the average ebullition estimate for
147 the whole lake should be much smaller. The ebullition calculated from the model was 10
148 $\pm 7\%$ (average ± 1 SD) higher than the uncorrected ebullition estimates.

149

150 **References**

- 151 1. Bastviken, D.; Cole, J.; Pace, M.; Tranvik, L. Methane emissions from lakes:
152 Dependence of lake characteristics, two regional assessments, and a global estimate.
153 *Global Biogeochemical Cycles* **2004**, *18* doi:10.1029/2004GB002238.
- 154 2. McAuliffe, C. Gas chromatographic determination of solutes by multiple phase
155 equilibrium. *Chem. Technol.* **1971**, *1*, 46-51.
- 156 3. Wiesenburg, D. A.; Guinasso, N. L. Equilibrium solubilities of methane, carbon
157 monoxide, and hydrogen in water and sea water. *J. Chem. Engineer. Data* **1979**, *24*,
158 356-360.
- 159 4. Cole, J. J.; Caraco, N. F. Atmospheric exchange of carbon dioxide in a low-wind
160 oligotrophic lake measured by the addition of SF₆. *Limnol. Oceanogr.* **1998**, *43*, 647-
161 656.

162

163

164

165 **Figure legends**

166 Figure S1. Map of the Pantanal showing the locations where measurements were made.

167 Some locations were very close to each other and are not separated with different

168 symbols at this scale. We thank Mr. Luiz Alberto Pellegrin for contributing the map.

169

170 Figure S2. Methane fluxes at different times in lake L1 based on short term

171 measurements (repeated sampling every 10th minutes for 40 minutes) in chambers partly

172 covering floating macrophytes (A) and over nearby open water just outside the

173 macrophyte belt (B). Measurements were made the same day and the time delay between

174 measurements in the two panels are due to practical constraints handling six replicate

175 chambers with frequent sampling. See Table S1 for lake information.

176

177 Figure S3. Total CH₄ flux versus maximum depth of the studied lakes. The line denotes a

178 non-linear regression ($\log_{10}(F) = -1.509 + 4.908z - 2.838z^2 + 0.4341z^3$; F is flux and z

179 depth, adjusted $R^2 = 0.40$). The dashed lines gives the 95% confidence interval.

Table S1. Overview of the studied lakes and some physicochemical characteristics including position, area during low water period (ALWP), max depth (z_{\max}), pH, alkalinity, sediment water content, organic carbon and organic nitrogen content, and C/N ratio. Mean values are reported. FW and DW denote fresh weight and dry weight, respectively, and nd indicates that no data are available.

Lake ID	Location	Position	ALWP	z_{\max}	Water chemistry			Sediment chemistry			C/N ratio
					pH	Alkalinity	Water content	Org. C	Org. N		
			km ²	m		mekv L ⁻¹	% of FW	% of DW	% of DW		
Belém	Ladario	57°29'40"W 18°59'26"S	nd	2.6	6.5	0.39	nd	nd	nd	nd	
Presa	Ladario	57°25'27"W 18°59'49"S	nd	2.7	6.6	0.50	32.0	2.85	0.24	12.0	
Bracinho	Ladario	57°32'63"W 19°00'25"S	nd	2.5	6.7	0.38	nd	nd	nd	nd	
Lobo	Ladario	57°36'90"W 18°57'11"S	nd	1.9	6.5	0.44	74.8	6.45	0.64	10.0	
Tereza	Ladario	57°26'28"W 18°57'38"S	nd	3.4	6.7	0.41	59.7	1.30	0.10	13.4	
L1	Ladario	57°32'53"W 19°01'17"S	0.06	2	5.9	0.56	92.0	10.88	0.91	12.0	
L2	Ladario	57°32'34"W 19°01'34"S	0.12	1.5	6.0	0.80	65.5	3.58	0.31	11.7	
L3	Ladario	57°28'23"W 19°01'50"S	0.35	2	6.3	0.44	50	1.52	0.14	11.0	
L4	Ladario	57°22'07"W 19°02'21"S	0.10	1.5	6.6	0.64	86.4	9.73	0.88	11.0	
TR	National Park	57°28'54"W 17°51'12"S	71.4	2.5	6.0	0.41	nd	0.75	0.07	10.7	
BB	National Park	57°23'33"W 17°50'15"S	36.3	1.2	6.2	0.33	nd	0.74	0.08	9.4	
N6b ¹	Nhumirim	56°37'57"W 18°58'01"S	0.12	nd	8.1	5.55	78.3	14.05	1.13	12.5	
N7a ¹	Nhumirim	56°38'46"W 18°58'25"S	0.10	0.5	10.7	16.94	33.3	5.76	0.48	12.1	
N8a ¹	Nhumirim	56°39'36"W 18°58'59"S	0.16	0.5	9.0	6.37	41.4	3.82	0.36	10.6	
N14	Nhumirim	56°39'22"W 18°59'41"S	nd	0.8	5.7	1.05	69.6	8.03	0.72	11.1	
N19a	Nhumirim	56°37'54"W 19°00'14"S	nd	0.8	5.3	0.42	65.2	8.80	0.78	11.3	

¹Lake N6b was very rich in organic matter as indicated by a dark brown water color. There were no macrophytes in this lake. Lakes N7a and N8a had very high carbonate levels and a green water color from highly abundant cyanobacteria. Macrophytes were absent.

Table S2. Overview over the results for each lake, including sampling date, number of flux measurements (n), average water temperature (T), methane concentration in the surface water ($[\text{CH}_4]_{\text{aq}}$), piston velocity (k_{CH_4}), diffusive flux, total flux, and percentage of total flux being ebullition. Note that k_{CH_4} is the apparent piston velocity for methane (see eg. 4 for how to calculate k for other gases from this value).

Lake	Date	n	T °C	$[\text{CH}_4]_{\text{aq}}$ μM	k_{CH_4} m d ⁻¹	Diffusive flux mmol m ⁻² d ⁻¹	Total flux mmol m ⁻² d ⁻¹	Ebullition %
Belém	15-Sep-2008	12	26	0.39	0.52	0.20	0.64	69
Presa	15-Sep-2008	11	27	0.5	1.09	0.86	1.69	49
Bracinho	16-Sep-2008	12	26	3	1.36	1.81	15.53	88
Lobo	16-Sep-2008	12	24	1.28	0.46	1.78	5.62	68
Tereza	17-Sep-2008	12	24	0.36	0.52	0.18	0.25	28
L1	5-Dec-2006	34	30	1.35	0.70	0.81	16.39	95
L2	7-Dec-2006	13	30	1.84	0.40	0.70	7.39	91
L3	7-Dec-2006	13	30	0.28	1.44	0.72	2.09	66
L4	7-Dec-2006	13	30	0.51	1.72	0.87	21.99	96
TR	26-Nov-2006	26	31	0.44	1.49	0.65	5.74	89
BB	26-Nov-2006	15	30.5	0.38	1.25	0.50	5.63	91
N6b	29-Nov-2006	10	27	1.32	0.36	0.48	12.45	96
N7a	29-Nov-2006	10	34	0.17	0.36	0.66	1.42	54
N8a	29-Nov-2006	12	29.5	0.83	0.83	0.69	5.17	87
N14	29-Nov-2006	8	29.5	0.58	0.67	0.39	20.68	98
N19a	29-Nov-2006	8	30	1.75	0.67	0.73	11.71	94
All		221				0.74	8.79	91

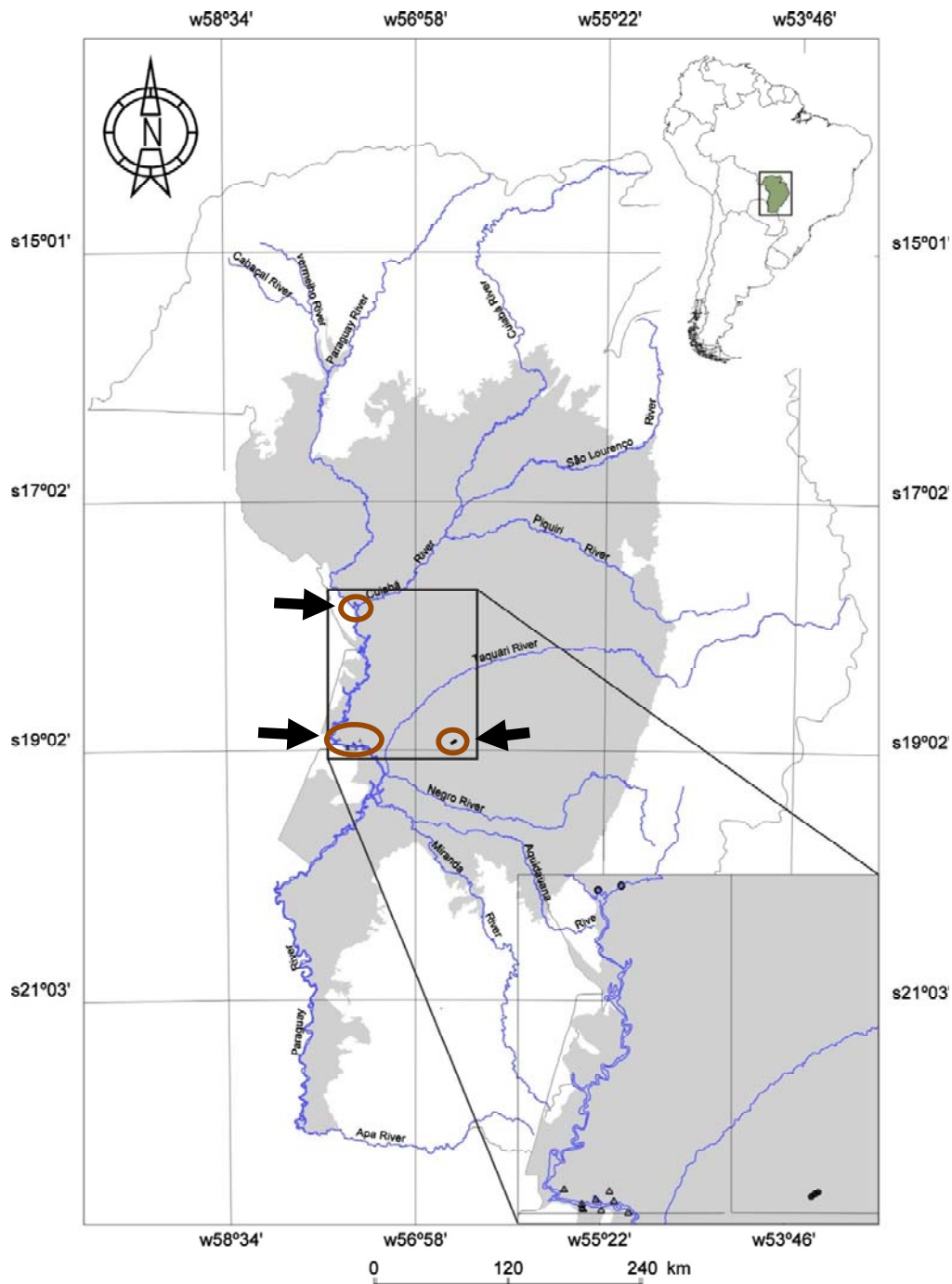


Figure S1. Map of the Pantanal showing the locations where measurements were made (marked by arrows and encircled in the large map and by points at individual sites at the insert). Some locations were very close to each other and are not separated with different symbols at this scale. We thank Mr. Luiz Alberto Pellegrin for contributing the map.

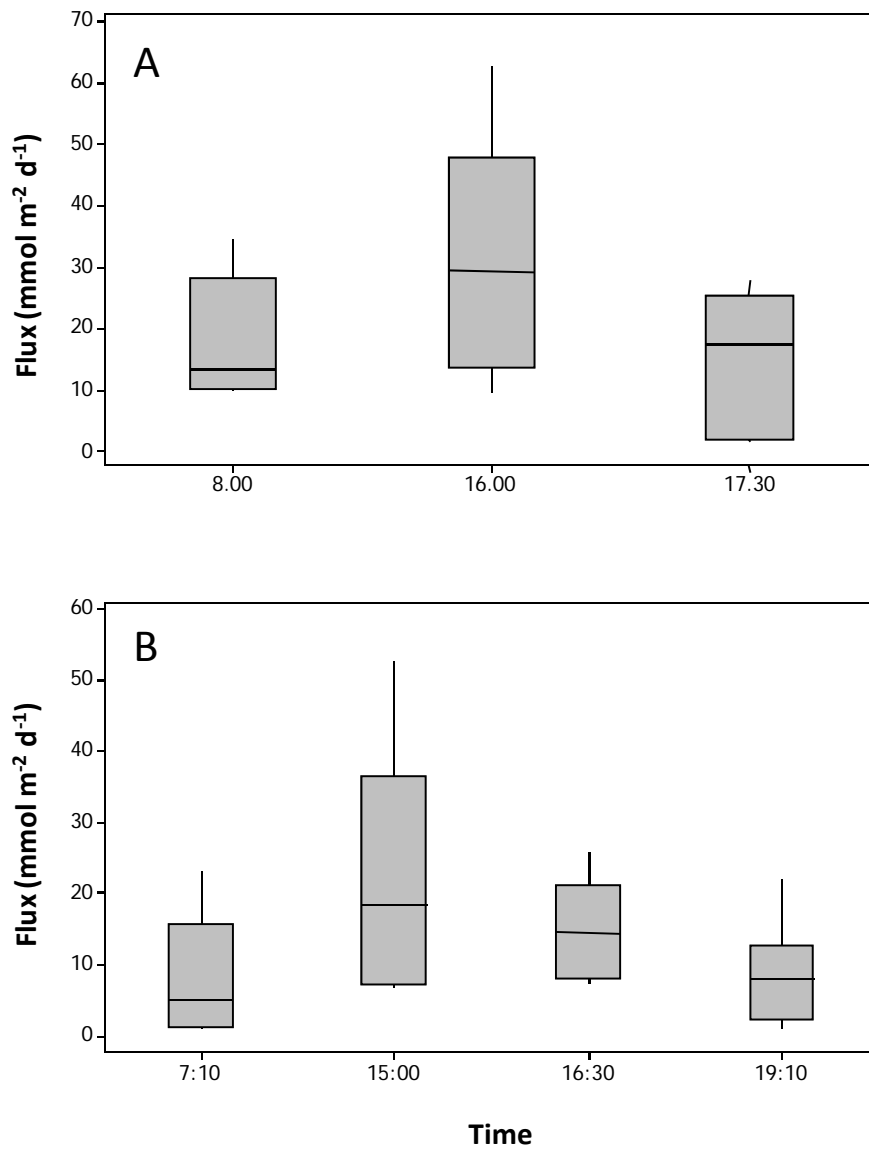


Figure S2. Methane fluxes at different times in lake L1 based on short term measurements (repeated sampling every 10th minutes for 40 minutes) in chambers partly covering floating macrophytes (A) and over nearby open water just outside the macrophyte belt (B). Measurements were made the same day and the time delay between measurements in the two panels are due to practical constraints handling six replicate chambers with frequent sampling. See Table S1 in Supporting Information for lake information.

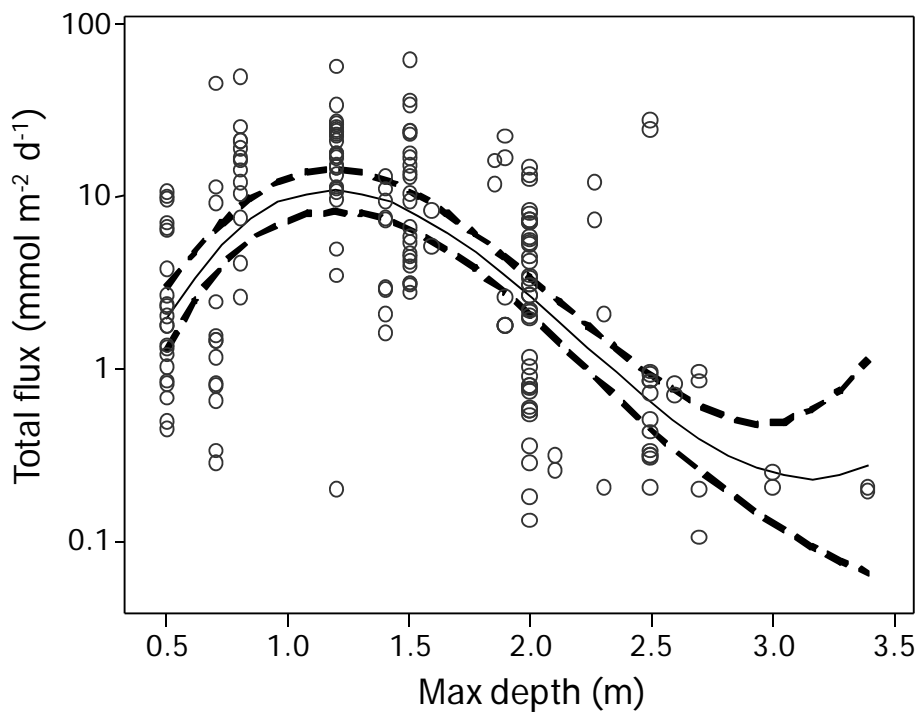


Figure S3. Total CH₄ flux versus maximum depth of the studied lakes. The line denotes a non-linear regression ($\log_{10}(F) = -1.509 + 4.908z - 2.838z^2 + 0.4341z^3$; F is flux and z depth, adjusted $R^2 = 0.40$). The dashed lines gives the 95% confidence interval.